Localized Contact Formation by Erythrocyte Membranes: Electrostatic Effects

N. E. Thomas and W. T. Coakley
School of Pure and Applied Biology, University of Wales, Cardiff CF1 3TL, Wales

ABSTRACT The topology of the contact seam of human erythrocytes adhered by dextran, an uncharged polymer, has been examined. Particular attention has been paid to the influence of electrostatic intermembrane interactions since their magnitude and range can be accurately estimated. Normal cells formed a continuous seam, whereas erythrocytes with pronase-modified glycocalices formed localized contact points on adhesion in 72 kDa dextran in buffered 145 mM NaCl. The dependence of the inter-contact distance λ on dextran concentration [D] over the range 2–6% w/v, was given by $\lambda = C[D]^{-0.62}$, where C was a constant. The index of [D] was independent of dextran molecular mass over the range 20 to 450 kDa. The inter-contact distance for pronase-pretreated cells in 6% w/v 72 kDa dextran increased from 0.78 to 1.4 μm as [NaCl] was reduced through the range 145 to 90 mM and the suspending phase was maintained at isotonicity by using sorbitol to replace NaCl. The formation and lateral separation of the contact points are discussed from the perspective of linear interfacial instability theory. The theory allows a quantitative explanation for the experimentally observed dependence of inter-contact distance and of disturbance growth rate on change in electrostatic interaction. The results suggest that the dominant wavelength, determining the inter-contact distance, is established on approaching membranes when the layers of cell surface charge are separated by a perpendicular distance of <14 nm (bilayer separation of 24 nm).

INTRODUCTION

The understanding of the physical chemistry of the processes that occur when cells approach each other has increased significantly in recent years as, on the biological side, more becomes known about the fine structure of the cell glycocalyx (Coakley et al., 1991; Fisher, 1993) and, on the physical side, inter-surface forces which are also important in cell interactions can be measured at surface separations on the order of nanometers (Fisher, 1993; Israelachvili and McGuigan, 1988; Patel and Tirrell, 1989).

The adhesion of erythrocytes by macromolecules and polymers has been widely studied as a model system in which to examine membrane interactions (Coakley et al., 1991, 1994; Fisher, 1993). Early work (Jan and Chien, 1973a,b; Katchalsky et al., 1959) identified the types of polymer and established the best experimental conditions with which to achieve adhesion. Later reports clarified the strength of cell adhesion (Buxbaum et al., 1982; Francis et al., 1987). Recent studies in this laboratory have concentrated on the topology of the seam of adhesion (Coakley et al., 1994). It has been shown that in one outcome of erythrocyte-erythrocyte adhesion the seam of contact is continuous (Skalak et al., 1981; Darmani and Coakley, 1990), whereas in a second outcome spatially periodic discrete local regions of contact are separated laterally by distances of the order of 1 μm (Coakley et al., 1985; Darmani and Coakley, 1990; Thomas et al., 1993, Sung and Kabat, 1994). The contact seam topology depends on the type of macromolecule mediating adhesion and on the extent to which the net normal pressure between the membranes has been modified, e.g., by enzymic pretreatments that reduce the cell glycocalyx surface coverage and/or reduce surface charge. Normal cells show spatially periodic contacts in polylysine (Thomas et al., 1993), whereas dextran forms a continuous adhesive seam in normal cells (Baker et al., 1993; Skalak et al., 1981) and forms spatially periodic contacts in pronase-pretreated cells (Baker et al., 1993; Darmani and Coakley, 1990). It has been shown that experimental procedures (e.g., polymer concentration change, glycocalyx modification) that increase the net attraction between cells reduce the inter-contact distance, whereas the inter-contact distance increases when the experimental procedure decreases the net attraction (Baker et al., 1993; Darmani and Coakley, 1990; Thomas et al., 1993; Coakley et al., 1994). This interest in contact topology was stimulated here by the ubiquitous appearance of localized point contacts in membrane adhesion in natural systems (Coakley and Gallez, 1989; Ward and Hammer, 1992). It parallels studies elsewhere of the contributions of the mechanical properties of receptors (Evans, 1985; Ward and Hammer, 1992) and of receptor movement (Ward and Hammer, 1992) implicit in the appearance of localized or continuous regions of membrane contact in vivo.

There is increasing experimental evidence that the occurrence of spatially periodic contacts when erythrocytes are drawn together under a net attractive interaction is consistent with the predictions of interfacial instability theory for destabilization of a thin liquid film (Coakley et al., 1994). The interfacial instability approach treats the two interacting membranes and the intermembrane water layer as a thin fluid film separated from two continuous phases (formed by the cytoplasms of the interacting cells) by transition zones,

Received for publication 30 December 1994 and in final form 5 July 1995.
Address reprint requests to Prof. W. T. Coakley, School of Pure and Applied Biology, University of Wales, Cardiff CF1 3TL, Wales. Tel.: 44-1-222-874287; Fax: 44-1-222-874305; E-mail: sabwtc@cardiff.ac.uk.

0006-3495/95/10/1387/15 $2.00

modeled as two-dimensional surface phases with appropriate physicochemical properties such as surface tension and surface charge (Gallez and Coakley, 1986). Knowledge gained from extensive studies in the field of colloid and interface instability (e.g., the approach and coalescence of bubbles and drops) (Ivanov, 1980) can then be applied to the behavior of interacting membranes (Dimitrov, 1982; Gallez and Coakley, 1986). The most general technique of stability analysis is to solve the equations of change for various perturbations of a specified initial state. This approach predicts not only the conditions for which instability will occur but also the rates of growth or decay of various disturbances (Miller, 1978). The deformation of a plane interface arising from a small perturbation can be expressed as a Fourier integral so that it suffices to determine the response of the system to simple sine or cosine disturbances. If a sine or cosine disturbance of any wavelength may grow then the system is unstable. In a system that is unstable over a range of wavelengths the wavelength with the fastest growth rate will dominate the instability growth.

Linear instability analysis, which is restricted to situations where the vertical displacement of the thin film surface is small compared to the thickness of the film, which again must be small compared to the wavelength of the disturbance, is applied below because of the guidance provided by its analytical solutions. Numerical solutions have been obtained by Gallez (1994) for the high-amplitude nonlinear dynamic behavior of an unstable aqueous film between a membrane and a solid substratum. In the linear analysis the development, with time t, of a single-frequency vertical disturbance (of initial amplitude ζ_o) of the surface of a cylindrically symmetrical thin film is described (Ivanov and Dimitrov, 1974) by $\zeta = \zeta_o(r) \cdot e^{\omega t}$, where r is a radial coordinate and ω (the sum of the real and virtual angular frequencies) is the complex angular frequency of the perturbation. If q, the real part of ω, is negative the disturbance will die out with time and the system is stable; if q is positive the displacement will grow exponentially and the interface is unstable. An initially flat film can become unstable through the growth of 1) a bending mode where the film profile becomes sinusoidal but remains of constant thickness or 2) a *squeezing mode* where the central plane of the film remains flat but spatially periodic variations in film thickness develop and grow (Wendel, Gallez and Bisch, 1981; Prevost, Gallez and Sanfeld, 1983). It is the latter spatial periodicity of film thickness that concerns us here.

Dimitrov (1982), as part of an analysis of squeezing mode stability for a thin film where the resistance to deformation was effected by bending elasticity B and membrane tension T constructed an equation for the component of the hydrodynamic pressure due to wave motion of amplitude ζ in the film. The expression reduced to the forms by Brochard and Lennon (1975) and Ivanov and Dimitrov (1974) for the cases where membrane tension and bending elasticity respectively were taken as zero. He obtained an expression for $\delta\zeta/\delta t$ from which a growth rate q was derived. Ruckenstein and Jain (1974) and Prevost and Gallez (1984) isolated conditions for bending and squeezing mode development for a charged aqueous film with tangentially immobile surfaces. Gallez and Coakley (1986) generalized these results for the case of a nonthinning aqueous layer between two interacting cells to give the following expression for q:

$$q = (h_f^3 k^2/24\eta)(2dP_T/dh - k^2\sigma_T - k^4 B) \qquad (1)$$

where h_f is the thickness of the undisturbed film, $k = 2\pi/\lambda$ with λ as the disturbance wavelength, η is the film viscosity, B is the membrane bending modulus. The total surface tension $\sigma_T = 2\sigma_S + \sigma_R + \sigma_A$, with σ_S as the pure surface tension and σ_R and σ_A as the contributions of repulsive and attractive interactions to surface tension (Gallez and Coakley, 1986). The total or net disjoining pressure P_T is the sum of the different normal membrane-membrane interaction pressures due, for instance, to the van der Waals (P_W), electrostatic (P_E), hydration (P_H), glycocalyx stereo-repulsion (P_R), and dissolved-macromolecule induced attraction (P_A). Equation 1 is identical to that obtained by Dimitrov (1982) except that surface tension σ_T is retained above whereas Dimitrov generalized to a membrane tension T. The criterion for a positive growth rate q and thus for the growth of a squeezing mode instability is that the second bracketed term of Eq. 1 should be positive. Therefore the squeezing mode *stability* criterion is given by

$$k^2\sigma_T + k^4 B - 2dP_T/dh > 0 \qquad (2)$$

It can be seen from criterion 2 that an aqueous intermembrane film is more likely to be stable when bounded by membranes of high surface tension and/or high bending elasticity. The stabilizing contributions of these parameters is reduced when k is small, i.e., at long wavelength ($k = 2\pi/\lambda$). The dependence on a intercellular water layer thickness h of a number of the contributions $P(h)$ to the net normal interaction pressure P_T can be described, excluding the case of van der Waals attraction, by terms of the form

$$P(h) = P_0 \cdot \exp(-h/L) \qquad (3)$$

where P_0 is a constant and L is a characteristic length for the interaction. When the pressure is repulsive (P_0 positive) the contribution of the first derivative of $P(h)$ terms as in Eq. 3 (or indeed for any function where repulsion increases with decreasing separation) to Criterion 2 is positive and therefore stabilizing. When the pressure is attractive the contribution is destabilizing. The derivative dP_T/dh of disjoining pressure is the second derivative of the net interaction potential, so that a high positive curvature of the interaction potential profile will be destabilizing. The explanation of how perturbations of a thin film of thickness h, at which the curvature of the interaction potential profile is positive, release potential energy to drive the spontaneous growth of a squeezing wave is discussed in more detail elsewhere (Coakley and Gallez, 1989).

The wavelength that will dominate disturbance growth in an unstable film is obtained by differentiating q (Eq. 1) with respect to k and setting $dq/dk = 0$ to give

$$\lambda = 2\pi[\sigma_T/dP_T/dh]^{0.5} \quad (4.a)$$

when B in Criterion 2 can be ignored compared with σ_T and

$$\lambda = 2\pi[B/dP_T/dh]^{0.25} \quad (4.b)$$

when σ_T can be ignored compared with B. When a squeezing wave of wavelength λ grows exponentially on the intercellular water layer it follows that the membrane will make localized contact at points separated by the distance λ along the membrane. If the formation of localized membrane contacts is to be described as an interfacial instability phenomenon then the experimentally determined inter-contact distances should be a measure of λ. It follows also from Eq. 4 that, where it is possible to quantify dP_T/dh at the onset of growth of the dominant instability, a log-log plot of λ against dP_T/dh should have a slope of -0.5 or -0.25 if membrane stretching or membrane bending respectively determine the outcome of the membrane interaction. The relative importance of stretching and bending resistance is of general interest in the understanding of membrane interactions (Lipowsky, 1995).

Criterion 2 gives the stability condition against squeezing wave growth for a film of fixed average thickness h (a nondraining film). When membranes approach each other under a net attractive interaction, drainage of intermembrane water will occur, so that the average film thickness decreases with time. The stability of both draining and nondraining thin aqueous layers between membranes was analyzed by Dimitrov (1982). The draining film treatment was confined to the case where the only interaction considered between electrically neutral lipid bilayers was the long-range van der Waals attraction. Dimitrov recognized, however, that significant insight into the instability process can be obtained from the simple solutions (Eqs. 1–4) available for the case of a nondraining film. These solutions will guide the discussion later in this paper.

It has been shown that the inter-contact distance depends on variables such as polymer concentration and the extent of enzyme pretreatment (Coakley et al., 1994) in a way that is consistent with the prediction that increased net attraction destabilizes the intercellular aqueous layer. It is difficult, however, to obtain good estimates of the combination of P_0 and L (Eq. 3) for those cases from the literature. Nevertheless, some attention is given here to the dependence of λ on polymer concentration where, for a fixed polymer molecular mass and therefore essentially fixed L (Eq. 3), P_A depends on polymer concentration through P_0. The main thrust of this paper is to investigate the adhesion outcome for variation in electrostatic interactions where L is known and P_0 can be reasonably estimated.

It has been known for some time that the increased electrostatic repulsion associated with a decrease in suspending phase ionic strength inhibits simple adhesion of normal erythrocytes suspended in a solution of the uncharged polysaccharide dextran of molecular mass 74 kDa (Jan and Chien, 1973a,b). The experiments reported below were carried out at a similar molecular mass of 72 kDa dextran. Erythrocytes were pretreated with pronase to an extent that increased net intermembrane attraction but retained sufficient surface charge to allow reasonably strong intermembrane electrostatic interaction. The suspending phase ionic strength was then changed to accurately modify L in Eq. 3.

The results show that inter-contact distance is sensitive to electrostatic repulsion in a way that is consistent with 1) the results of previous experiments in which intermembrane interaction was modified by different means and 2) with the predictions of interfacial instability theory. Estimates of the cell separation at which the dominant instability is established and of the growth rate of that instability (Eq. 1) are obtained.

MATERIALS AND METHODS

Erythrocyte preparation

Human erythrocytes were obtained by finger prick into 10 ml of phosphate-buffered saline (PBS; i.e., 145 mM NaCl and 5 mM phosphate, pH 7.32) containing, to avoid cell crenation, 0.1 mg · ml^{-1} bovine serum albumin (BSA) (BDH Ltd.). The cells were centrifuged at 1000 × g for 1 min. The supernatant and buffy coat were removed by aspiration. The cells were resuspended and washed in the above PBS/BSA to give a concentration of 3.5×10^7 cells · ml^{-1} when finally resuspended in PBS/BSA. Experiments were completed within 2 h of finger puncture.

Pretreatment of cells with pronase and exposure to dextran

Volumes (typically 1 ml) of the cell suspension were added to equal volumes of pronase (0.4 mg · ml^{-1} or 1.0 mg · ml^{-1}) (Boehringer Mannheim) in PBS to give the final enzyme concentrations quoted in the Results. The cell/pronase preparations were held at room temperature for a known time with occasional shaking. The samples were then diluted 5× in PBS, centrifuged at 1000 × g for 1 min, and washed in 10 ml PBS before final resuspension in 1.0 ml PBS. This suspension was then mixed with 1.0 ml 72 kDa dextran (Sigma, Ltd.) in PBS and held at room temperature for 30 min with occasional shaking. The polymer concentrations quoted in the Results were the concentrations in the final solutions. Where required the polymer-treated cells were fixed in suspension by addition of 1 ml of 6% w/v glutaraldehyde (EM grade, Sigma, Ltd.) in PBS and held at room temperature for 10 min. The fixed cells were washed and resuspended in PBS.

In the first of two separate experiments designed to search for any influence of cell manipulation on the reproducibility of membrane contact seam topology, four 1.0-ml samples were taken from the bulk blood suspension (at point A, Fig. 1) and subsequently processed separately as described above. In the second experiment a 4.0-ml volume of cell suspension in PBS/BSA was mixed with an equal volume of enzyme solution. The cell/pronase preparations were held at room temperature for a known time with occasional shaking. The sample was split into four 2-ml samples (at point B, Fig. 1) and processed in parallel from that point onward.

Cell-suspending phases of reduced ionic strength consisted of 5 mM phosphate buffer, 120 mM NaCl with 60 mM sorbitol (pH 7.24), or 90 mM NaCl with 101 mM sorbitol (pH 7.11). The human erythrocyte membrane is impermeable to sorbitol (Freedman and Laris, 1981). The suspending media were designed to maintain constant cell volume and constant intra-

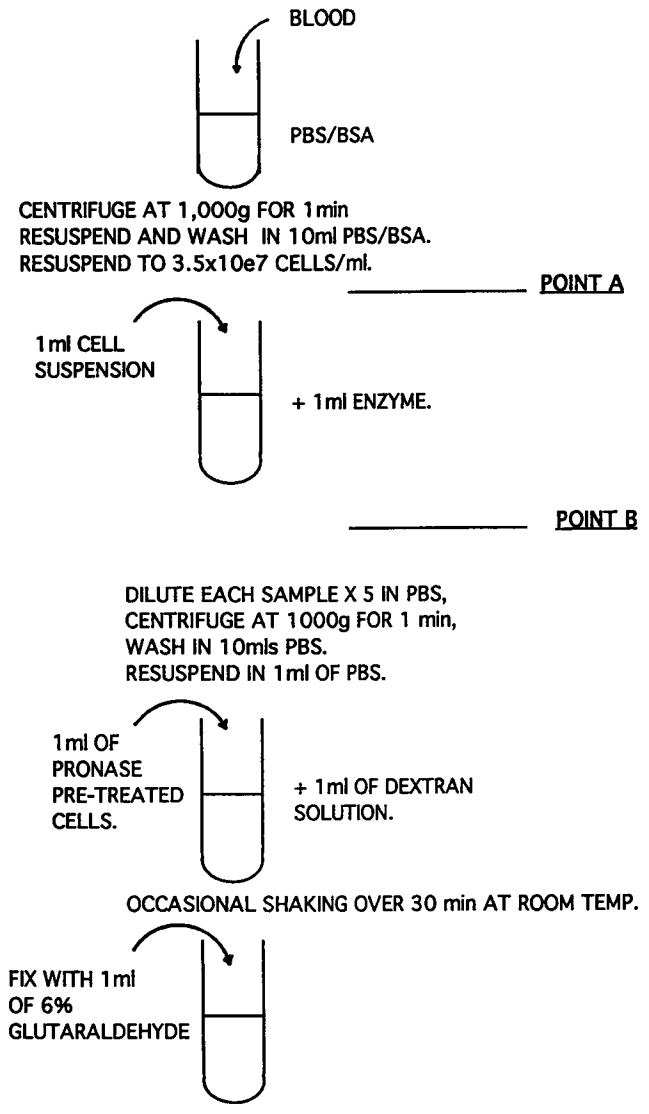

FIGURE 1 Experimental procedure for preparation of blood suspension, treatment with enzymes and exposure to dextran. Point A shows where, in one experiment, four 1.0-ml samples of blood were taken and subsequently processed in parallel. Point B shows where in one experiment a 4.0-ml sample of blood suspension was incubated with 4.0 ml of enzyme solution, and four 2.0-ml samples were subsequently processed in parallel.

cellular chloride concentration when the extracellular chloride concentration was varied. Chloride and hydrogen ions are in Donnan equilibrium across the erythrocyte membrane (Hoffman and Laris, 1974). Consequently, any reduction of extracellular chloride ion concentration would alter the intracellular pH and the hemoglobin charge. Chloride ions and water would then leave the cell. To avoid the resulting cell volume and transmembrane potential change the extracellular pH was adjusted, as previously described (Hoffman and Laris, 1974; Doulah et al., 1984) The osmolality of the solutions was measured with a freezing point depression osmometer (Advance Instruments).

Light and electron microscopy: scoring of adhesion and of lateral contact separation

Dextran-treated cells (fixed or unfixed) were examined by differential interference contrast microscopy with an oil immersion ×63 objective (Nachet). The percentage of adhered cells was calculated from light microsopy examination of 200 cells per sample. The percentages of the adhered cells in edge to edge contact with partial overlap (Pa), fully overlapping adhered cells with parallel membrane contact (P), cells with spatially periodic contacts of Long (> 1.8 μm), Med (1.8 μm > Med > 1.2 μm), and Short (Short < 1.2 μm) lateral separations were also calculated.

For electron microscopy preparation glutaraldehyde-fixed cells were centrifuged at 1000 × g for 1 min, resuspended in 3% glutaraldehyde in PBS, and held at 4°C for 30 min. The cells were washed and resuspended overnight in 0.1 M phosphate buffer. The cells were then washed and post-fixed in phosphate-buffered OsO_4 (140 mM NaH_2PO_4, 96 mM NaOH, 45 mM glucose, and 4 μM OsO_4) for 1 h at 4°C. Cells were dehydrated by serial washing and resuspension in increasing concentrations of ethanol (50%, 70%, 90%) for 15 min each at 4°C and finally in 100% ethanol for 30 min at room temperature. Samples were transferred to suspension in 100% Spurr resin, through a series of Spurr/ethanol steps, over 1 week. The final overnight infiltration was in 100% Spurr with rotation in a fume cupboard. Fresh Spurr was added and the sample was rotated for 24 h before polymerizing aerobically overnight in an oven at 60°C. Sections (60 nm) were then cut and examined using a Jeol Jem 100S TEM at 80 kV. The lateral inter-contact separation distance along the seam of cell adhesion was measured from transmission electron micrographs. An average inter-contact distance was calculated for each seam from 10 agglutinates (approximately 15 seams in total). An overall average inter-contact distance for the regime under which the cells had been exposed to polymer was then calculated.

Electrophoretic velocity measurements

Cell suspension (1.0 ml) (3.5×10^7 cells · ml^{-1}) was diluted 10× in PBS, centrifuged for 1 min, and resuspended in 10 ml of PBS. This suspension was loaded into a 40-mm-long rectangular cross section (10 mm × 1 mm) glass electrophoresis cell in a modified (Sutherland and Pritchard, 1979) Mark II cytophorimeter (Rank Brothers, Bottisham, Cambridge) and exposed to a 5-mA current. The velocity of enzyme-pretreated cells, measured in the stationary layer, was expressed as a percentage of the velocity of control erythrocytes to give an index of the amount of remaining cell surface charge (Schnebli et al., 1976).

Calculation of electrostatic repulsive pressure

The interactions involved in the close approach of two erythrocyte membranes will be considered as those of two glycocalyx-coated interfaces separated by an aqueous electrolyte. The glycocalyx consists principally of the charge-carrying glycophorins, which reach out about 5 nm from the bilayer, and the band 3-associated 7 kDa polysaccharides, which reach out 10–14 nm (Viitala and Jarnefelt, 1985).

The general term for the electrostatic repulsion between two plane surfaces separated by a distance h in a symmetrical monovalent electrolyte of counterion concentration n_0 ions · m^{-3} is given by (Hiemenz, 1986)

$$P_E(h) = 64 n_0 k_B T \gamma_o^2 \exp(-h/\kappa^{-1}) \quad (5)$$

where k_B is Boltzmann's constant and T is absolute temperature. The distance h for calculation of $P_E(h)$ in the particular case of a glycocalyx is taken to be the separation distance between the outer edge of the glycophorins, which protrude about 5 nm from the bilayer (Viitala and Jarnefelt, 1985), because the sharp fall in potential profile with distance from the bilayer begins in that region (Donath and Voigt, 1983). At a temperature of 25°C and an electrolyte ionic strength I, κ^{-1} and γ_o, respectively, are given by (Hiemenz, 1986)

$$\kappa^{-1} = 4.31 \times 10^{-10} \times (2I)^{-0.5} \quad (6)$$

and

$$\gamma_o = (\exp(e\psi_0/2kT) - 1)/(\exp(e\psi_0/2kT) + 1) \quad (7)$$

where e is the electronic charge and ψ_0 is the electric potential at the surface.

An estimate of the erythrocyte surface potential, calculated as the zeta potential of a sphere of uniform surface charge density, gives a value of 14 mV for cells in 145 mM saline (Haydon and Seaman, 1967). It has frequently been observed that the electrophoretic mobility of blood cells suspended in solutions of neutral polymers in saline is significantly higher than that expected for cells in suspending phases of elevated viscosity (Baumler and Donath, 1987). This result led to the suggestion that the surface potential of cells in dextran is higher than that of cells in saline (Brooks, 1973a). More recently (Baumler and Donath, 1987; Donath et al., 1989) the high electrophoretic mobility of cells in dextran has been attributed to the reduced viscosity (compared to the bulk phase viscosity) of a dextran depletion layer at the cell surface, thus removing the need for the assumption of a high cell surface potential in dextran. Treatments of how the volume distribution of charge within the glycocalyx influences erythrocyte electrophoretic mobility suggest that the potential fall with distance from the bilayer is small through the charged region of the glycocalyx (Donath and Voigt, 1983) and that the potential at the edge of the charged volume is smaller than the classically calculated value of 14 mV (Levine et al., 1983). Within the limitations of present models of the glycocalyx and its spatial charge distribution the value of ψ_0 at the edge of the glycophorins (i.e., 5 nm from the bilayer) will be taken below to be 7 mV for normal erythrocytes in 145 mM NaCl.

RESULTS

Enzyme pretreatment of cells

Experiments were carried out to characterize surface charge removal by different pronase concentration/time regimes. Fig. 2 shows that the charge removal (calculated from electrophoretic velocity change) produced by 0.5 mg/ml pronase initially increased with time but did not depend detectably on exposure time in the range 10–30 min, in agreement with earlier experiments (Baker et al., 1993; Darmani and Coakley, 1990). The figure also shows that the charge removal for a 20-min exposure did not depend strongly on pronase concentration in the range 0.2–0.5 mg/ml.

Light and electron microscopy observations showed that the contact seam of normal (not pretreated with enzyme) erythrocytes in 6% w/v 72 kDa dextran was continuous and parallel (Fig. 3a). The contact seam of pronase-pretreated cells showed local spatially periodic regions of cell contact (Fig. 3 *b*). The inter-contact distances, the percentage of cells that adhered during exposure to dextran, and the electrophoretic velocity changes for cells treated with 0.2 or 0.5 mg/ml pronase for 20 min before exposure to 6% w/v 72 kDa dextran in PBS are shown in Table 1. The result that exposure to 0.2 or 0.5 mg/ml pronase for 20 min before suspension in 72 kDa dextran removed similar amounts of charge but gave marked differences in inter-contact distance (Fig. 2, Table 1) is consistent with an earlier conclusion that nonelectrostatic consequences of pronase pretreatment of a glycocalyx make a significant contribution to changes in membrane interaction between cells suspended in 450 kDa dextran solutions in 145 mM NaCl (Darmani and Coakley, 1990).

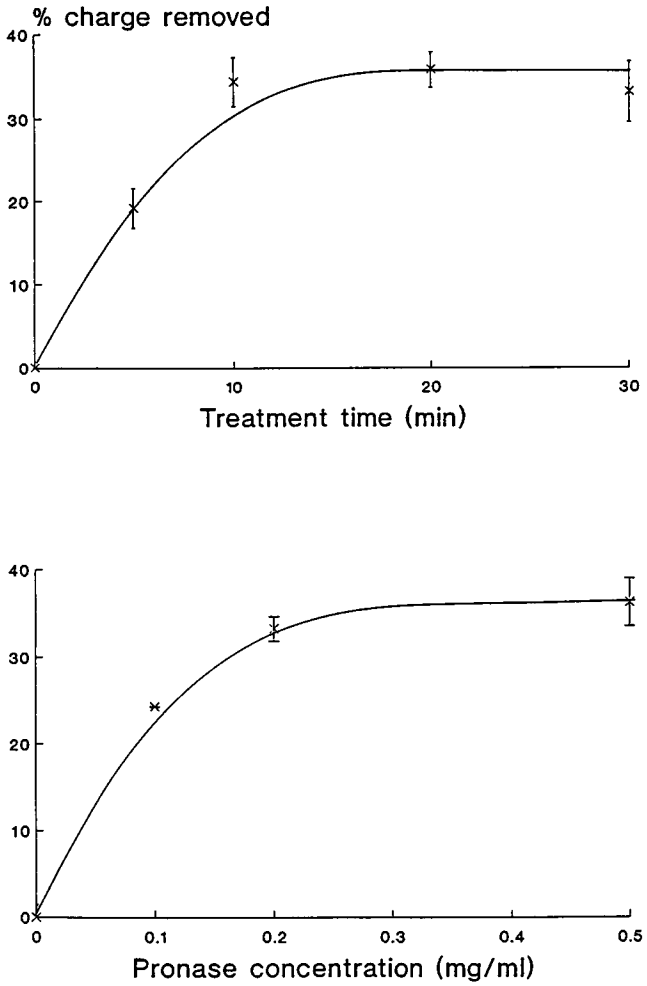

FIGURE 2 The dependence of percentage surface charge loss (based on electrophoretic velocity measurements) on (*a*) treatment time with pronase at a concentration of 0.5 $mg \cdot ml^{-1}$ (the 95% confidence limits are based on the means of 3–14 samples at the different times); and (*b*) pronase concentration at a treatment time of 20 min. The two 95% confidence limits shown are based on the means of three sets of samples, each processed and measured on the same day.

A previous qualitative assessment of the inter-contact distances in pronase-pretreated erythrocytes over a wide range of experimental conditions showed that the separations were among the shortest for 6% w/v 72 kDa dextran (Baker et al., 1993). Based on the results of Fig. 2 and Table 1, pretreatment with 0.5 mg/ml pronase for 20 min was chosen as a standard preparatory step in the examination of the effect of ionic strength on inter-contact distance in the present study because this regime 1) gave a short inter-contact distance of 0.96 μm in 6% w/v dextran in PBS, thus providing scope to detect an increase in inter-contact distance with increasing electrostatic repulsion; 2) retained sufficient surface charge to expect significant change in electrostatic repulsion with ionic strength (Table 1); and 3) gave an electrophoretic velocity change (surface charge

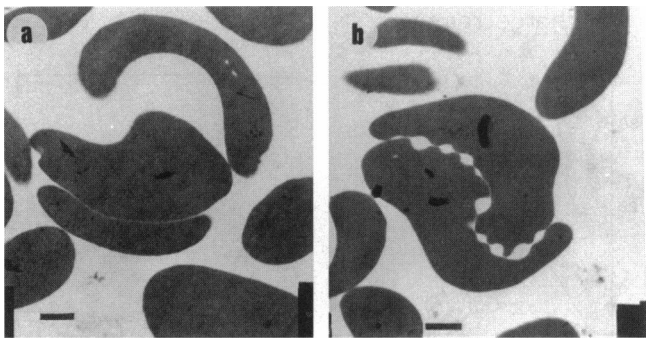

FIGURE 3 Transmission electron micrographs showing, for cells exposed to 6% w/v 72 kDa dextran in PBS, (*a*) the plane parallel contact seam in normal cells and (*b*) the spatially periodic contact seams of cells pretreated with 0.5 mg/ml pronase for 20 min. The bars represent 1 μm.

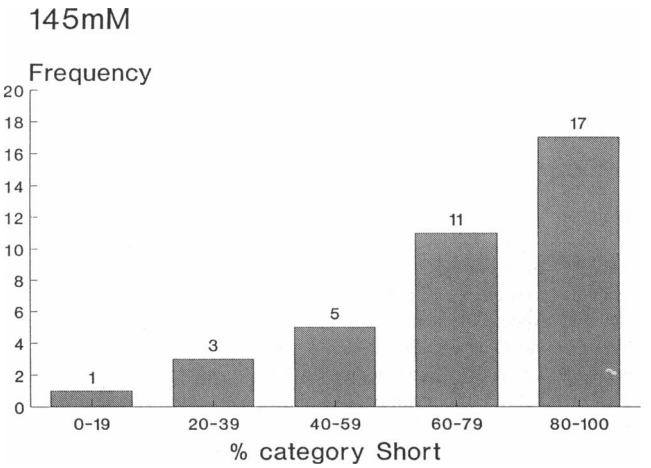

FIGURE 4 Frequency histogram of the percentages of adhered cells per sample showing Short inter-contact distances after pretreatment with 0.5 mg/ml pronase for 20 min and exposure to 6% 72 kDa dextran for 30 min in PBS. The total number of samples examined was 37.

removal) that was not sensitive to small variations in the pronase concentration/time regime (Fig. 2).

The contact seam of pronase-pretreated erythrocytes exposed to 6% w/v 72 kDa dextran in buffered 145 mM NaCl

The average inter-contact distance of 0.96 μm for cells pretreated with 0.5 mg/ml pronase before exposure to 6% w/v dextran (Table 1) implies a high incidence of Short category inter-contact distances in the sample examined. As part of a check on the reproducibility of indices of contact separation from different experiments the percentage of contact seams showing Short inter-contact distance was determined for different samples. A histogram of the frequency of occurrence of different percentages of Short distance is shown in Fig. 4 for 37 samples, each prepared on a different day. The incidence of Short distance was greater than 60% for most (28/37) of the samples. However, low incidences of Short distances were also recorded (Fig. 4). There was no correlation between measured electrophoretic velocity change and incidence of Short inter-contact distance in 17 samples for which both parameters were determined (15 of the 17 values of electrophoretic velocity decrease lay in the range 28–42%).

TABLE 1 Changes in inter-contact distance, electrophoretic velocity, and the percentage of adhered cells for samples treated with different concentrations of pronase for 20 min and then exposed to 6% w/v of 72 kD dextran in PBS

Pronase concentration (mg/ml)	Mean contact separation ±95% conf limits (μm)	Adhered cells (%) ±95% conf. limits	Decrease in electrophoretic velocity (%)
0	N.A.	21 ± 11	0
0.2	2.31 ± 0.31	38 ± 23	33 ± 6
0.5	0.96 ± 0.08	48 ± 6	36 ± 12

The 95% confidence limits for (1) the inter-contact separation were based on 15 measurements from single samples; (2) the adhered cells were based on 4, 4 and 16 measurements respectively for the increasing pronase concentrations, and (3) the electrophoretic velocity were based on measurements from three samples.

Experiments were carried out to determine whether the variation reflected in Fig. 4 arose from small differences in the manipulation of the cells in the course of experiments or was associated with day-to-day variation in the properties of the blood samples. Four separate samples prepared from the bulk cell suspension (point A in Fig. 1) were subsequently processed normally and examined by light microscopy. A second experiment was carried out by preparing four separate 2.0-ml samples from an 8-ml cell/enzyme preparation at point B of Fig. 1. The means of the data in Fig. 4 and of the two sets of four samples were 65.0%, 65.8%, and 83.0%, respectively, and their standard deviations were 26.3%, 13.5%, and 11.0%, respectively. The standard deviations of the sets of four measurements were similar to each other and were of the order expected from a Poisson distribution of counts when, typically, about 100 of the 200 cells examined per sample had adhered to another cell and 60–80% of the contact categories were short. A variance ratio test for the data of Fig. 4 and a pooled variance for the two sets of data based on four points each implied ($p < 0.05$) that a significant component of the variation in the data of Fig. 4 was related to day-to-day variation rather than to variation within experiments. For this reason where change in inter-contact distance with experimental varible is presented below the data are shown, where possible, as a change of response on that day, i.e., the presentation is essentially of paired data, eliminating day-to-day variation.

Ionic strength effect on inter-contact distance of pronase-pretreated cells in 72 kDa dextran

There was no detectable difference between the average percentages of pronase-pretreated cells that had adhered

after exposure to 6% w/v dextran in suspending medium containing 145, 120, or 90 mM NaCl (Table 2).

The electron microscope measurements of Table 2 show that the average inter-contact distance increased for decreasing ionic strength of the suspending medium. Light microscopy observations of the cell clumps showed that the mode adhesion category in 145 mM NaCl was the Short-separation spatially periodic contact (Fig. 5). The percentage of adhered cells in the Short category was significantly smaller ($p < 0.01$) for cells in 120 mM NaCl with sorbitol, and the distribution had shifted to longer separation categories (Fig. 5). The mode category for cells in buffered 90 mM saline with sorbitol was plane parallel contact (P) without localized contacts.

The paired comparisons of Fig. 6 confirm the significance of the decrease in Short category as the NaCl concentration is decreased and the increase in parallel contacts in 90 mM NaCl.

The contact seams of two samples examined after suspension in 70 mM NaCl with sorbitol had no short lateral separations, whereas 80% and 91% of the agglutinates had continuous parallel contacts. In a set of nine samples where the NaCl concentration was 60 mM there were five results in which no seam had short contacts and more than 90% of all agglutinates formed continuous seams. Four of the nine samples showed a high incidence (48% < Short < 72%) of Short lateral separation contacts. Two of these four samples were part of sets of experiments carried out at different NaCl concentrations on single batches of cells. The incidence of Short contacts in the 90 mM samples from those sets was zero. Such significant increases in Short category with decreasing [NaCl] did not occur in any of the 15 series of concentration experiments carried out in the higher (145–90 mM) range. We return to the occurrence of this short wavelength disturbance in the Discussion. Erythrocytes in 50 mM NaCl with sorbitol showed a stomatocytic form (Doulah et al., 1984; Glaser, 1982). These more rounded cells made adhesive contact in 6% dextran, but the contact did not spread, making it impossible to investigate contact seams in salt concentrations below 60 mM.

TABLE 2 Electron microscopy determinations of the average inter-contact distance for cells that were pretreated with 0.5 mg/ml pronase and exposed to 6% w/v 72 kD dextran in buffered 145 mM NaCl, in buffered 120 mM NaCl with 30 mM sorbitol, or in buffered 90 mM NaCl with 110 mM sorbitol

NaCl Concentration (mM)	145	120	90
Average inter-contact distance (μm)	0.80 ± 0.06 0.75 ± 0.04	0.89 ± 0.08 0.95 ± 0.08	1.42 ± 0.12 1.39 ± 0.16
Adhered cells (%)	46% ± 4%	42% ± 9%	49% ± 5%

The results were obtained from two separate experiments. The results include a 95% confidence range for each average separation value. The average percentage of cells (with 95% confidence limits) that had adhered in suspension is also shown for 31, 6, and 15 samples in 145, 120, and 90 mM NaCl, respectively.

Chloride ion concentration and contact formation

In a series of experiments the incidence of the different adhesion categories was established for cells suspended in

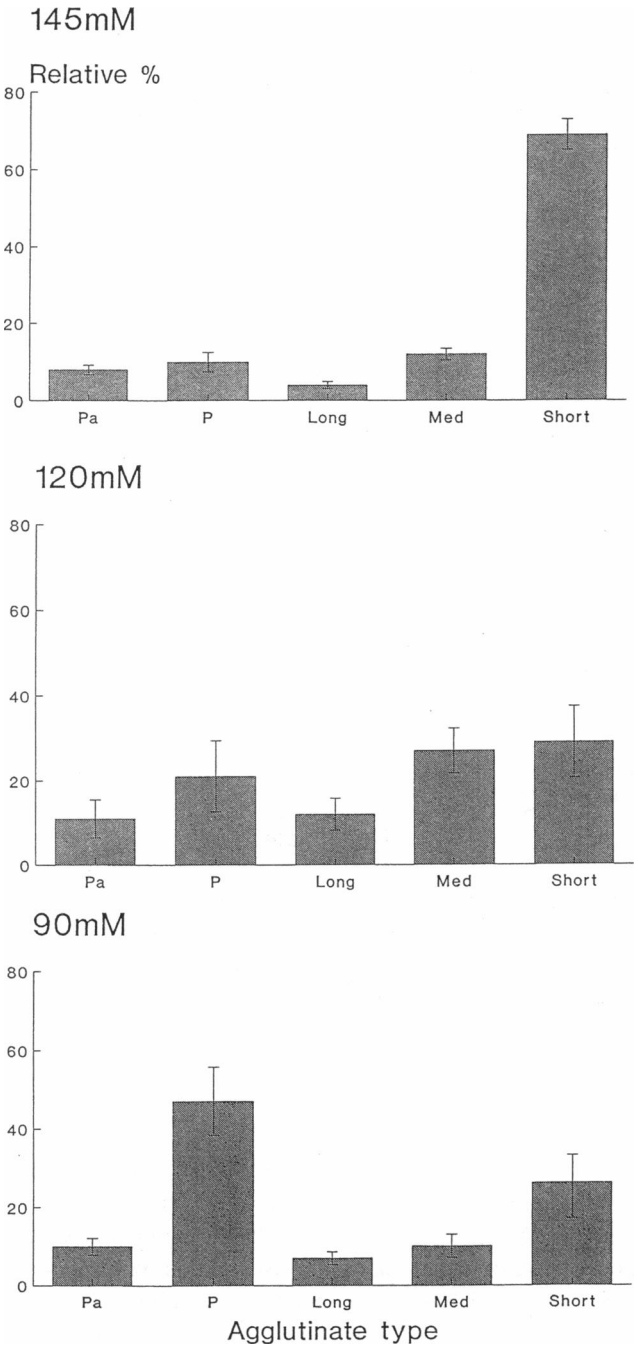

FIGURE 5 Mean percentage frequency of occurrence (±1 standard error of the mean) of different forms of contact formed when cells pretreated with 0.5 mg/ml pronase for 20 min adhered on exposure to 6% w/v 72 kDa dextran in buffered 145 mM NaCl (top), in buffered 120 mM NaCl with 30 mM sorbitol or in buffered 90 mM NaCl with 110 mM sorbitol. The results are means from 32 samples in 145 mM NaCl, 6 samples in 120 mM NaCl, and 15 samples in 90 mM NaCl. The contact categories were Pa (parallel seams in cells in edge-edge contact), P (parallel seam in cells in rouleaux), Long (>1.8 μm), Med (1.8 μm > Med > 1.2 μm), and Short (<1.2 μm) inter-contact distances.

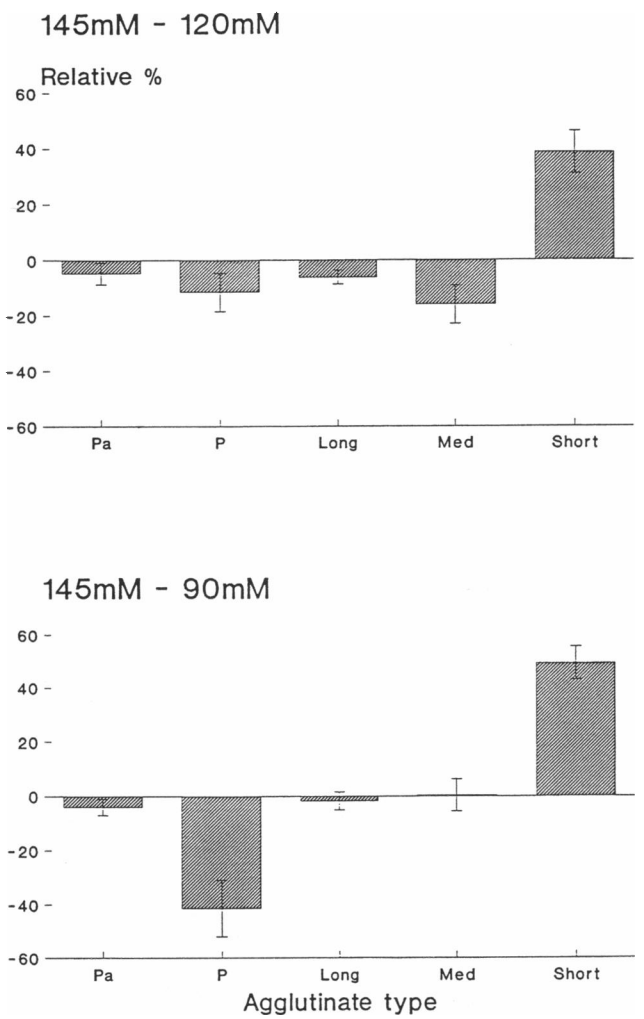

FIGURE 6 Means (±1 standard error of the mean) of four paired comparisons of the percentage frequencies of occurrence of contacts formed in pronase-pretreated cells exposed to dextran in buffered 145 mM NaCl with cells in (*a*) buffered 120 mM NaCl with 30 mM sorbitol and (*b*) buffered 90 mM NaCl with 110 mM sorbitol. The experimental conditions and contact categories are as in Fig. 5.

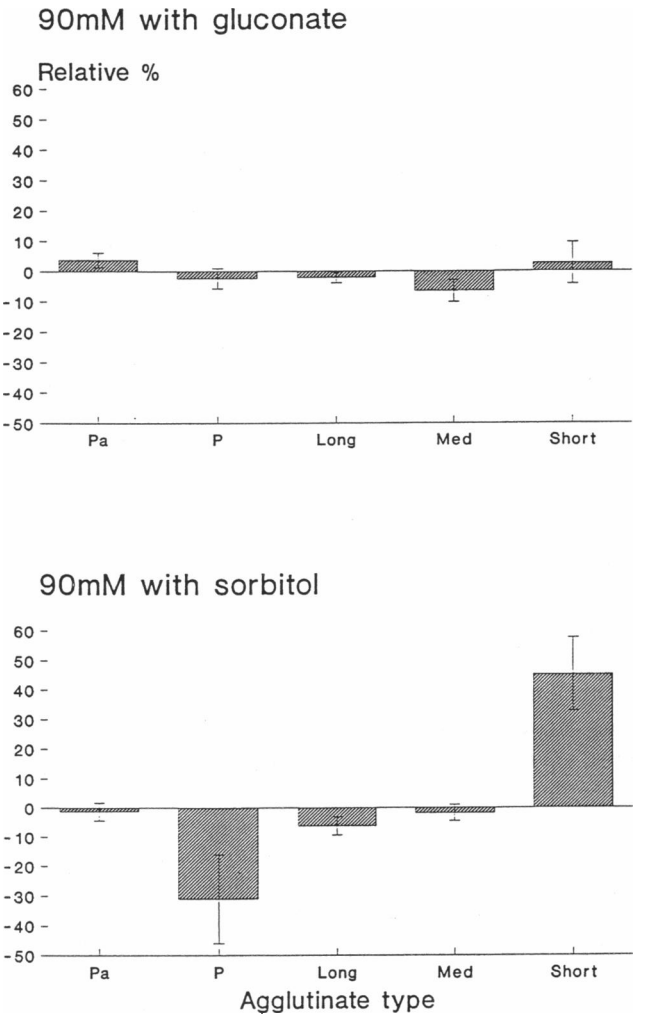

FIGURE 7 Means of six paired comparisons of the percentages of different contact categories formed in pronase-pretreated cells exposed to dextran in buffered 145 mM NaCl with cells in buffered 90 mM NaCl made isotonic with sodium gluconate or with sorbitol. The error bars indicate one standard error of the mean.

buffered 145 mM NaCl and in buffered 90 mM NaCl made isotonic either with sodium gluconate or with sorbitol. Fig. 7 shows the differences obtained from paired comparisons of the results in suspending phases containing either 145 mM or 90 mM NaCl. The incidence of short inter-contact distances is lower and continuous parallel contact is higher in the low ionic strength 90 mM NaCl with sorbitol, in a manner that is consistent with the results of Figs. 5 and 6, whereas the incidences of the different categories for cells in 145 mM NaCl and in 90 mM NaCl with 55 mM sodium gluconate are essentially the same for both suspending phases. This result shows that the different categories of contact result from ionic strength change rather than from the chloride ion concentration dependence (Hoffman and Laris, 1974) of erythrocyte transmembrane potential.

Influence of concentration of 72 kDa dextran on adhesion of pronase-pretreated cells

Pronase-pretreated cells (0.5 mg/ml for 20 min) were exposed to different concentrations of 72 kDa dextran. The percentage of suspended cells that adhered under the different conditions are shown, together with the average inter-contact distance, in Table 3. The relative frequencies of the different forms of contact of the adhesion seams are shown in Fig. 8, and the electron micrographs of Fig. 9 are representative examples of the contact seams in the different dextran concentrations examined.

The dependence of lateral contact spacing in pronase-pretreated cells on the concentration of 72 kDa dextran (Table 3) is shown together with earlier data for cells in 450 kDa and 20 kDa dextran from Baker et al. (1993) in the log-log plot of Fig. 10 *a*. The slope of the best fit straight

TABLE 3 The average inter-contact distances and the percentages of adhered cells (with 95% confidence limits) for pronase-pretreated cells in different concentrations of dextran in PBS

[Dextran] (% w/v)	2	4	6
Ave. inter-contact distance (μm)*	1.93 ± 0.21	1.24 ± 0.18	0.97 ± 0.11
Adhered cells (%)‡	46 ± 18	53 ± 15	42 ± 11

*The measurements of inter-contact distances were obtained from an experiment based on a single blood sample. The average distances were based on about 15 determinations of inter-contact distance from electron micrographs, as described in Materials and Methods, for each dextran concentration.

‡The percentages of adhered cells were calculated from counts in experiments carried out with fresh blood on three different days.

line through the eight data points was −0.62, with a 95% confidence interval of 0.05, giving a relationship of the form

$$\lambda = C \cdot [D]^{-0.62} \quad (8)$$

where C is an unknown function of both molecular mass and pronase pretreatment conditions. The exponent of [D] is independent of molecular weight over a molecular mass range of 20–450 kDa. The pronase pretreatments for experiments with the different molecular mass polymers were selected so that the inter-contact distance data were spread over the range from the upper experimental limit of about 3 μm (set by the size of the erythrocyte) to the lower limit of about 0.8 μm, toward which the inter-contact distance tends for cells in dextran (Baker et al., 1993; Darmani and Coakley, 1990). Because the pronase pretreatments for the data subsets of Fig. 10 *a* were not the same, it follows that the common dependence of λ on [D] does not imply that inter-contact distance is independent of molecular mass at a fixed dextran concentration. For comparison, Fig. 10 *b* shows a log-log plot of inter-contact distance against polymer concentration for erythrocytes adhered by exposure to 228 kDa polylysine (Thomas et al., 1993). The slope of the plot is −0.50. (The data from Baker et al., 1993, and Thomas et al., 1993, included in Fig. 10, have not previously been presented in log-log form.)

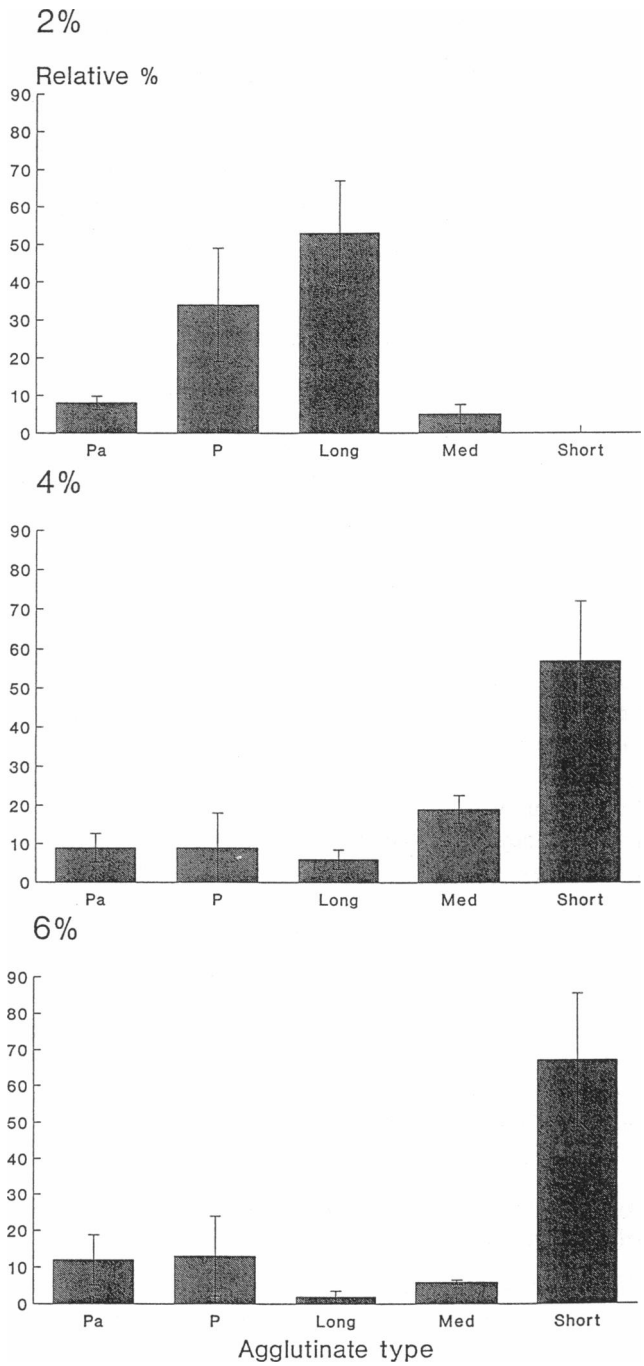

FIGURE 8 Mean percentages (±1 SEM, three experiments) of different categories of contact formed when cells pretreated with 0.5 mg/ml pronase adhered on exposure to 2%, 4%, and 6% w/v 72 kDa dextran in buffered 145 mM NaCl.

DISCUSSION

Modifications of membrane interaction

Jan and Chien (1973b) showed that modification of electrostatic interaction through reduction of suspending phase ionic strength for normal cells or through surface charge depletion by pretreatment of cells in 145 mM NaCl with neuraminidase markedly affects the probability of adhesion by 74 kDa dextran. Whereas the adhesion probability for cells in 145 mM NaCl with 6% w/v dextran increases with pronase pretreatment in the present study (Table 1), the more prolonged pretreatments result in an adhesion probability that is essentially independent of cell interaction modifiers such as dextran concentration at fixed ionic strength (Table 3) or ionic strength changes at fixed dextran concentration (Table 2) over the ranges of these variables tested. The principal effect of the above interaction modifiers was to change the inter-contact distance.

In establishing the interfacial instability framework within which this result will be discussed we will first examine the magnitude of the two stabilizing terms $k^2\sigma_T$ and k^4B in Criterion 2. k ($= 2\pi/\lambda$) is calculated for λ = 1.5

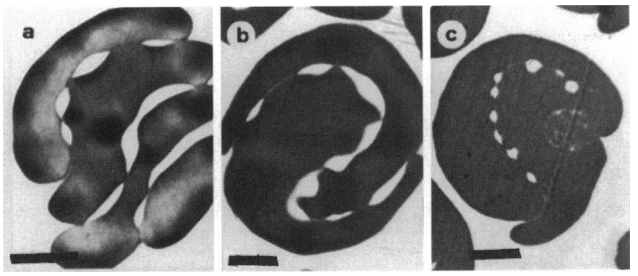

FIGURE 9 Electron micrographs of typical contact patterns for enzyme-pretreated cells exposed to (*a*) 2%, (*b*) 4%, and (*c*) 6% 72 kDa dextran. The bars represent 2 μm.

μm because this wavelength was taken as an upper limit for the disturbances that could grow for the Table 1 pretreatment and dextran solutions employed through most of this study (Table 2). Published values for the erythrocyte membrane bending modulus B range from 4×10^{-19} J to 1.4×10^{-19} J (Evans, 1983; Peterson et al., 1992). Its value is taken here as 3×10^{-19} J. The literature does not provide such a narrow range for estimates of σ_T. McIver and Schurch (1982) showed that incorporation of erythrocyte glycophorins into a lipid bilayer changed the interfacial tension from 5×10^{-3} N m^{-1} to 10^{-6} N m^{-1} and that the lower value was also the interfacial tension of intact erythrocytes. They suggested that the magnitude of the interfacial free energy appropriate for the thermodynamic analysis of interactions at biosurfaces depended on the location of the relevant interface. They associated the higher order of magnitude (5×10^{-3} N m^{-1}) with processes involving the bilayer properties. The values of $k^2_{\lambda=1.5\ \mu m}\ \sigma_T$ based on the σ_T estimates of McIver and Schurch (1982) are 9×10^{10} and 2×10^7 J m^{-4} for lipid bilayer and intact erythrocyte, respectively, whereas the estimate of $k^4_{\lambda=1.5\ \mu m}\ B$, at 10^8 J m^{-4}, lies between these values.

Interfacial instability and polymer concentration effect on inter-contact distance

Polymer concentration, the only constraint varied in obtaining the intercontact spacings for each subset of data in Fig. 10, influences the stability criterion 2 through its contribution P_A to P_T in dP_T/dh. This contribution, taken to be of the form of Eq. 3 or essentially of any form that has a constant P_0 multiplied by a concentration-independent term that increases with decreasing separation, depends on how polymer concentration is related to P_0. The interpretation of the indices -0.62 and -0.50 in the context of Eq. 4 therefore depends crucially on this relationship. A linear relationship would favor a surface tension controlled instability mechanism (Eq. 4a), whereas a relationship in which disjoining pressure increased with the square of polymer concentration would emphasize bending control (Eq. 4b). The relationship will now be considered.

Dextran (Chien et al., 1977) and polylysine (Katchalsky et al., 1959) adsorb to erythrocytes. Cross-linking (bridging)

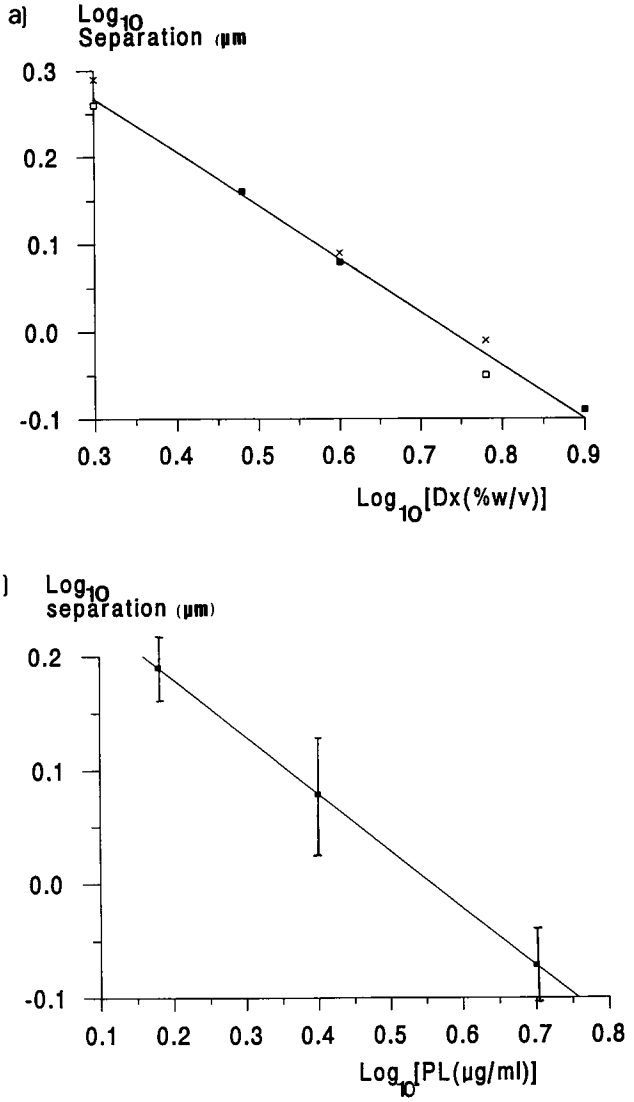

FIGURE 10 The polymer concentration dependence of the the average inter-contact distance: (*a*) Cells pretreated with 0.5 mg/ml pronase for 60, 20, or 15 min and exposed to (×) 20 kDa, (■) 72 kDa, or (□) 450 kDa dextran, respectively. (The 72 kDa data are from the present work; the remaining data are from Baker et al., 1993). (*b*) Normal erythrocytes exposed to 228 kDa polylysine (Thomas et al., 1993). The error bars are 95% confidence limits on wavelength determinations from a single suspension.

by dextran (Jan, 1979) and polylysine (Marra and Hair, 1988) can, it has been argued, bring about adhesion of erythrocytes and particles, respectively. Polymer depletion layers at a particle surface, such as shown for erythrocytes in dextran (Donath et al., 1989), can induce particle flocculation. Indeed, Snowden et al. (1991) experimentally separated polymer bridging and depletion flocculation mechanisms for silica particles suspended in aqueous solutions of an adsorbing polymer. In discussing the relationship between polymer concentration and P_0 we therefore need to consider polymer cross-linking for polylysine and both (van Oss et al., 1990) polymer cross-linking and depletion flocculation mechanisms for dextran-induced adhesion.

The attractive depletion flocculation interaction potential between particles is directly proportional to the osmotic pressure of the suspending polymer solution (Vincent et al., 1986). The relationship between dextran concentration and osmotic pressure can be calculated from published virial coefficients (Vink, 1971) for dextrans of the weight average molecular mass of about 40 kDa and 500 kDa, respectively. These molecular weights cover much of the 450–20 kDa range of the data in Fig. 10 *a*. The calculations show that for the threefold dextran concentration increase (2–6% w/v) in Fig. 10 *a* the osmotic pressure increases are 9.5 ($= 3^{2.05}$) and 4.9 ($= 3^{1.45}$) -fold for T500 and T40, respectively. Because the relationship between osmotic pressure and dextran concentration therefore depends on molecular size it follows that the slopes of the log-log plots for the different molecular weight subsets in Fig. 10 *a* should depend on molecular mass if the adhesion mechanism was simply related to depletion flocculation potential. This expectation is not borne out by inspection of the data of Fig. 10 *a*.

Cross-bridging of particles by adsorbed particles is a complex phenomenon, which in addition to an attractive interaction can involve stereo-repulsion (Luckham and Klein, 1990) and surface free energy changes (Rossi and Pincus, 1988) due to the polymer adsorption and further electrostatic interactions for polyelectrolytes (Marra and Hair, 1988). Mica force balance studies and theoretical treatments for irreversibly adsorbed polymers provide semi-quantitative guidance on the outcome of these interactions. As polymer coverage of apposed surfaces increases it becomes more difficult for an adsorbed polymer to encounter a vacant adsorption site on the second surface, so that for a given surface separation there is a coverage at which attraction is a maximum (Rossi and Pincus, 1988; Luckham and Ansarifar, 1990). For the above irreversible adsorption case the surface coverage at thermodynamic equilibrium is independent of the concentration of dissolved polymer. In contrast, because dextran (Brooks, 1973b; Chien et al., 1977) and polylysine (Katchalsky et al., 1959) adsorb *reversibly* to erythrocytes, surface coverage depends on concentration of free polymer in solution. The adsorption of 70 kDa dextran to erythrocytes essentially increases in a linear manner with polymer concentration up to 6% w/v and more slowly thereafter, without reaching a limit, even at 20% w/v dextran (Brooks, 1973b; Chien et al., 1977). Electrophoretic mobility measurements (Thomas et al., 1993) imply that polylysine adsorption increases asymptotically toward a saturation level at polycation concentrations significantly higher than the 1.0–5.0 μg/ml values required for the lateral separations of Fig. 10 *b*. Thus because surface coverage tends to asymptotic values with increasing polymer concentration and attraction grows to a maximum value with surface coverage and then declines (Rossi and Pincus, 1988), it follows that the contribution of cross-linking to the attractive disjoining pressure will grow at a decreasing rate as polymer concentration is increased. Therefore it may be concluded that the -0.62 and -0.50 regression coefficients would not move toward the -0.25 value associated with a bending modulus controlled mechanism were it possible to plot wavelength against disjoining pressure in Fig. 10.

To summarize this section: Despite the fact that the concentration of polycation required for adhesion is about $\times\ 10^{-4}$ that of dextran (Fig. 10) the -0.50 and -0.62 indices for the relationship between inter-contact separation and polymer concentration are quite similar. The indices are compatible in sign and magnitude with predictions of interfacial instability theory for the dependence of intercontact separation on the gradient of disjoining pressure. Consideration of a depletion flocculation mechanism for dextran provides some support for bending control, but an associated prediction that regression coefficients should be molecular mass dependent is not borne out by experiment. For a polymer cross-linking (bridging) mechanism the indices are more consistent with tension rather than bending control.

Electrostatic effects and the value of *h* for growth of the dominant disturbance

The cells exposed to different NaCl concentrations in the present study had all been pretreated to the same extent with pronase and been exposed to the same concentration of 72 kDa neutral polymer. We therefore assume that the only variation, with change in electrolyte concentration, in Criterion 2 above arises from electrostatic effects. One source of variation comes from the electrostatic repulsive contribution (P_E, Eq. 5) of the remaining surface charge to the net interaction P_T. Change in electrolyte concentration also modifies the negative contribution σ_{DL} of the electrical free energy of formation of the double layer to the membrane tension σ_T (Prevost and Gallez, 1984) where

$$\sigma_{DL} = -[\epsilon\kappa\psi_0^2/4\pi]\cdot[\sinh(\kappa h) - \kappa h]/[\cosh(\kappa h) - 1] \tag{9}$$

and ϵ is the dielectric constant of the electrolyte.

The contribution of the gradient of P_E to $-dP_T/dh$ (Criterion 2) is shown for different values of h in Fig. 11 *a*. The ionic strengths of the 145, 120, and 90 mM NaCl solutions buffered by 5 mM phosphate were taken as 0.15, 0.125, and 0.095 with κ^{-1} values (Eq. 6) of 0.787, 0.862, and 0.989 nm, respectively. The distance h for calculation of P_E and of σ_{DL} was the separation distance between the outer edge of the glycophorins, which protrude about 5 nm out of the bilayer (Viitala and Jarnefelt, 1985). The surface potential ψ_0 (Eqs. 7 and 9) for charge-reduced, pronase-pretreated cells in 145 mM NaCl was approximated as 4 mV, the product of the part of surface charge surviving pronase pretreatment (0.6; Fig. 2) and the control cell surface potential (7 mV; Materials and Methods). The ψ_0 estimate was changed with $I^{-0.5}$ (Hiemenz, 1986) for the small potentials and the limited changes in ionic strength of this work.

Fig. 11 *b* shows the dependence of $k^2_{\lambda=1.5\ \mu m}\ x\sigma_{DL}$ on h. The value of $k^4_{\lambda=1.5\ \mu m}$ xB is also shown in Fig. 11 as a guide to the magnitude of terms influencing Criterion 2.

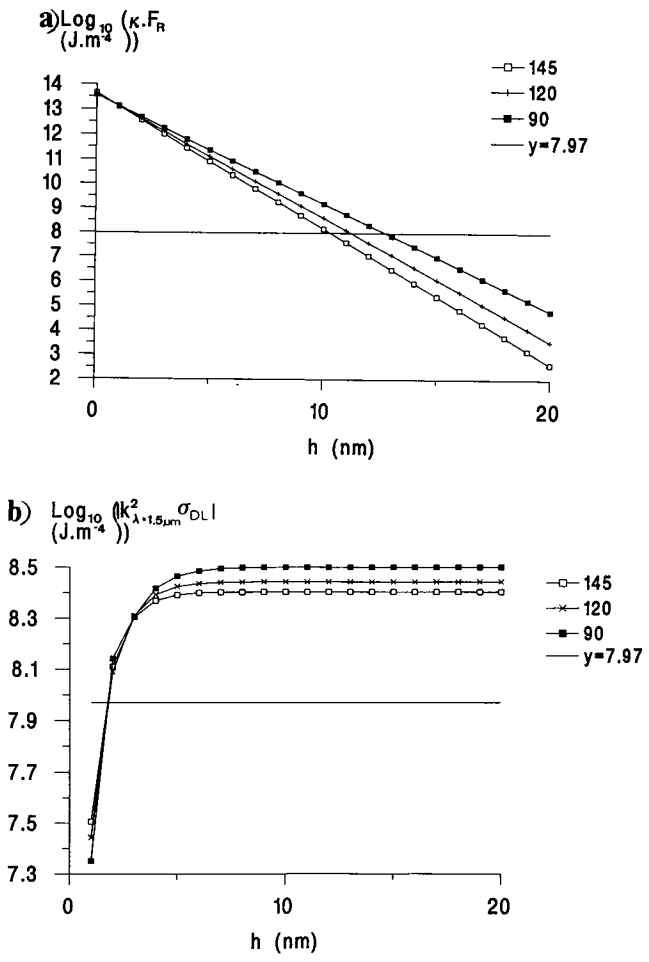

FIGURE 11 The dependence of (*a*) the contribution ($2\kappa.P_E$) of the gradient of the electrostatic repulsion pressure to $-2dP_T/dh$ (Criterion 2) and (*b*) $|k^2_{\lambda=1.5\,\mu m}\,x\sigma_{DL}|$ on separation h for cells in 145, 120, and 90 mM NaCl. The horizontal line gives the value of $k^4\lambda = 1.5\ \mu m$ xB (Criterion 2).

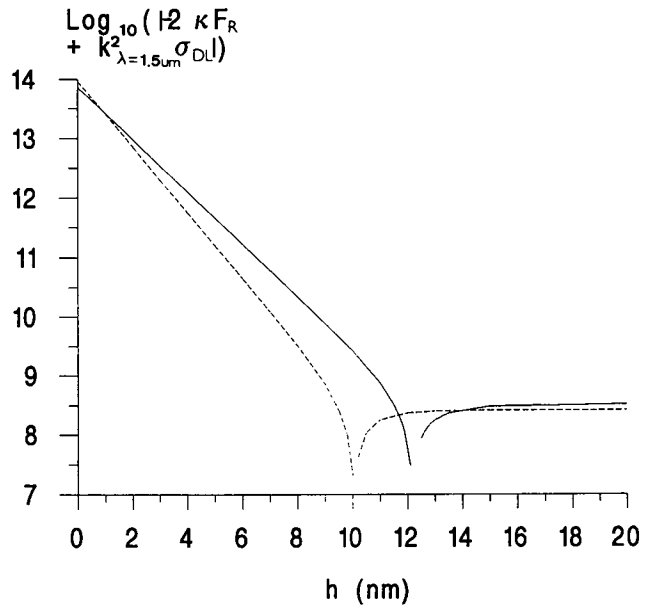

FIGURE 12 The modulus of the sum, EI, of the electrical contributions $k^2_{\lambda=1.5\,\mu m}\,x\sigma_{DL}$ and $2\kappa.P_E$ to Criterion 2 for NaCl concentrations of 145 (– – –) and 90 (——) mM as a function of h. The change from positive stabilizing to negative destabilizing values of EI occurs, for increasing h, at 10 nm for 145 mM and at 12.1 nm for 90 mM NaCl.

The modulus of the sum, EI, of the two electrical contributions $k^2_{\lambda=1.5\,\mu m}\,x\sigma_{DL}$ and $2\kappa{\cdot}P_E$ to Criterion 2 is shown in Fig. 12. Inspection of Figs. 11 and 12 shows that for cells in 145 mM NaCl EI makes a net destabilizing contribution, through the negative effect of $k^2_{\lambda=1.5\,\mu m}\,x\sigma_{DL}$, to Criterion 2 for values of $h > 10$ nm and a net stabilizing contribution, through the positive effect of $2\kappa{\cdot}P_E$, for values of $h < 10$ nm. The corresponding change for cells in 90 mM NaCl occurs at $h = 12.1$ nm. We noted (Results) that a high incidence of short lateral separations of local contacts in a number of samples in 60 mM NaCl occurred against the trend toward plane parallel contacts in lower ionic strength media. As ionic strength is decreased the destabilizing contribution of σ_{DL} (Eq. 9) will increase and dominate the stabilizing repulsive interaction as h ranges above 12 nm. The net increase in destabilizing contribution as ionic strength is decreased from 90 to 60 mM is $5 \times 10^7\ J \cdot m^{-4}$ at $h = 18$ nm. This contribution may explain the occurrence (Results) of instability in some of the samples examined at the lowest NaCl concentration (60 mM).

The experimental observation that when the NaCl concentration was decreased to 90 mM more than half of the contact seams in adhered cells showed continuous (category Pa or P) rather than localized contact (Fig. 5) and that the two samples at 70 mM (Results) showed less than 7% localized contact (category Long or Med only) implied that a threshold NaCl concentration ($[NaCl]_t$) exists where electrostatic repulsion is sufficient to ensure that Stability Criterion 2 is not breached during adhesion. If a value for $[NaCl]_t$ is assumed the change $\Delta(EI)$ in the electrostatic contribution to Criterion 2 at higher salt concentrations can be calculated for any value of h.

Rather than confine consideration of the relationship between intercontact separation, physical properties of the membrane, and dP_T/dh to the specific forms of Eq. 4 we will examine how the experimental data relate to the following more general equation of the form of Eq. 4, i.e.,

$$\lambda = 2\pi(S)^M(\Delta(EI))^{-M} \qquad (10)$$

S in Eq. 10 becomes σ_T or B, and M becomes 0.5 or 0.25 in Eqs. 4a and 4b, respectively. $\Delta(EI) = \Delta(|-2dP_E/dh + k^2\sigma_{DL}|)$, rather than dP_E/dh alone, features in Eq. 10 because the inclusion of σ_{DL} signals the values of h for which the net electrostatic contribution becomes more destabilizing as ionic strength decreases (Fig. 12).

Values of M and S obtained from linear regressions of $\log(\lambda)$ (data of Table 2) against $\log(\Delta(EI))$ for a $[NaCl]_t$ range from 90 to 60 mM and a separation range of 13–2 nm are given in Table 4. A requirement placed on $[NaCl]_t$ was that it should be less than 90 mM. The choice of the upper

TABLE 4 Paired values of M and S derived for $\lambda = 2\pi(S)^M(\Delta(EI))^{-M}$ (Eq. 10) from a log-log plot of the inter-contact distances of Table 2 against change in the electrostatic contribution to the stability criterion (Criterion 2) for different values of the threshold NaCl concentration for stability ($[NaCl]_t$) and the glycocalyx separation h

h (nm) $[NaCl]_t$ (mM)	2	4	6	8	10	12	13
89						0.189 1.3×10^{-28}	0.208 7.4×10^{-26}
88			0.201 7.2×10^{-24}	0.216 2.7×10^{-22}	0.231 4.7×10^{-21}	0.254 2.9×10^{-19}	
87		0.217 1.3×10^{-20}	0.239 2×10^{-18}	0.259 5.5×10^{-17}	0.28 8×10^{-16}	0.313 3.9×10^{-14}	
85	0.233 6.6×10^{-18}	0.275 6.9×10^{-14}	0.276 1.7×10^{-14}	0.339 1.1×10^{-10}	0.374 1.3×10^{-9}	0.429 3.9×10^{-8}	
83	0.274 1.8×10^{-13}	0.327 6.9×10^{-10}	0.371 4.1×10^{-8}	0.417 7.6×10^{-7}	0.469 7.8×10^{-6}	0.555 2×10^{-4}	
80	0.329 3×10^{-9}	0.403 7×10^{-6}	0.469 3.5×10^{-4}	0.541 5.4×10^{-3}	0.659 1.5×10^{-1}	0.798 1.43	
75	0.415 7.2×10^{-5}	0.53 0.1	0.643 3.89				
60	0.653 104					2.61 3×10^{7}	

limit on h was guided by the reversal of sign of the net electrostatic contribution to stability at around 12 nm (Fig. 12). This separation is within the 21 nm ($3 \times R_g$, where R_g is the radius of gyration of 72 kDa dextran (Snabre et al., 1985)) reach of surface cross-linking by polymers (Patel and Tirrell, 1989).

Table 4 shows that M has values around 0.25 as $[NaCl]_t$ and h are decreased from 88 to 85 mM and from 12 to 2 nm, respectively. The S value of 2.9×10^{-19} when $[NaCl]_t$ is 88 mM and $h = 12$ nm is close to published values of the bending modulus B (Evans, 1983; Peterson et al., 1992).

M has values around 0.5 as $[NaCl]_t$ falls from 83 to 75 mM and h decreases from 12 to 4 nm (Table 4). The associated values of S (Table 4, Fig. 13) fall within the range 5×10^{-3} N m^{-1} to 10^{-6} N m^{-1} suggested by McIver and Schurch (1982) for the interfacial tension of erythrocytes.

S and M values for $[NaCl]_t = 60$ mM and $h = 12$ nm are included in Table 4 to show that for a situation where the value of M, at 2.61, has no physical meaning in the context of the linear interfacial instability theory, the associated S value of 3×10^7 has no physical meaning in terms of bending modulus or surface tension.

Fig. 13 illustrates the constraints placed on the values of S associated with different values of M by the prescribed choices of $[NaCl]_t$ and h in Table 4. Table 4 and Fig. 13 then show that there are conditions, compatible with experimental results, that give indices for a relationship between wavelength and the electrostatic contribution to the stability condition which accommodate either index of Eq. 4 and that the restricted ranges of S associated with each of these indices contain realistic values for the membrane bending modulus or for membrane tension. For electrostatic interaction then, within the limits of linear theory and the assumption of a fixed film thickness for the growth of instability, Table 4 allows the instability mechanism but cannot on its own favor bending or tension controlled instability mechanisms.

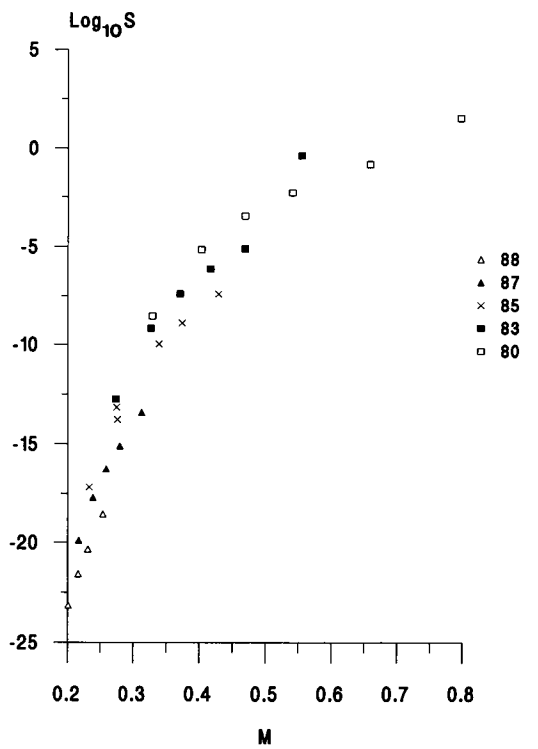

FIGURE 13 The clustering of the paired values of M and S derived for $\lambda = 2\pi(S)^M(\Delta(EI))^{-M}$ (Eq. 9) from a log-log plot of the inter-contact distance measurements of Table 2 against change in the electrostatic contribution to the stability criterion (2) for different values of ($[NaCl]_t$) and h. The data are identified here for the different values of $[NaCl]_t$. Corresponding values of h can be obtained through M and $[NaCl]_t$ in Table 4.

The rate of growth of the dominant disturbance

An estimate of q, the rate of evolution of the dominant disturbance, can be obtained from Eq. 1: $q = 1.64(h_f^3/\lambda^2\eta) \cdot (2dP_T/dh - k^2\sigma_T - k^4 B)$. The film thickness h_f is

taken as (h + 10) nm because h for the electrostatic interactions was measured from the edges of the glycophorins that protrude from the bilayer by 5 nm. Consider first where (Table 4) $M = 0.254$ and $S = 2.9 \times 10^{-19}$ J for $[NaCl]_t$ = 88 M and h = 12 nm. The average, $\Delta(EI)$, of the values of $\Delta(EI)$ associated with the different ionic strengths of Table 2 was 1.7×10^8 J m^{-4} for these values of $[NaCl]_t$ and of h. Taking $\lambda = 1$ μm, $\eta = 0.001$ kg m^{-1} s^{-1} for the viscosity of the aqueous intermembrane layer, $h_f = 22$ nm and $\Delta(EI) = 1.7 \times 10^8$ J m^{-4} to serve as the second bracketed term on the right-hand side of Eq. 9, gives $q = 1.75$ s^{-1}. The time ($3/q$) for growth of a disturbance is then 1.7 s. This time is larger than, but of the same order as, the measured time of 0.48 s to complete cell doublet formation in pronase-pretreated erythrocytes agglutinating in 2% w/v 450 kDa dextran (Darmani and Coakley, 1990). For a case where M = 0.50 and $S = 10^{-4}$ N m^{-1} ($[NaCl]_t$ = 80 mM and h = 7 nm), the value of $\Delta(EI) = 5 \times 10^{10}$ J m^{-4} and $3/q$ is 7 ms. That local membrane contact can occur in vivo in times consistent with the above values for q is shown when vesiculation occurs in sea urchin egg within a small part of 1 s of initiating the acrosome reaction (Dan, 1967). Vesiculation in the acrosome reaction involves the formation of hybrid vesicles produced by regular local contact formation and fusion between apposed sperm head and outer acrosomal membranes (Russell et al., 1979).

CONCLUSIONS

Inter-contact distance increases when ionic strength change increases the repulsive component of the electrostatic contribution to the interfacial stability criterion. This result is consistent with previous studies where different procedures modified inter-membrane interactions. The experiments reported here for different ionic strength suspending phases provide, for the first time, a system for which the characteristic length L of the contact separation determining interaction is accurately known. Instability theory calculations, informed by experimentally determined limits on saline concentration, allow relationships between measured inter-contact distance and the electrostatic contribution to the stability criterion which accommodate bending or tension controlled instability mechanisms but do not, as yet, select against either. The growth of the disturbance that determines lateral separation occurs when the glycophorins of interacting membranes are separated by distances that may be less than but are unlikely to be significantly greater than 12 nm. The growth rates of dominant instabilities, calculated from electrostatic interactions, are consistent with experimental observations of cell adhesion times.

The index for the dependence of inter-contact distance on dextran concentration was independent of molecular mass and was similar to the index for dependence of inter-contact distance on polycation concentration in other work where red cell adhesion was achieved with lower ($\times 10^{-4}$) polymer concentrations. Uncertainties in the current understanding of the relationship between polymer concentration and disjoining pressure hampers unequivocal assignment of the stability control to membrane tension or membrane bending mechanisms.

The support provided for an interfacial instability mechanism in achieving synchronous localized close approach of opposite membranes emphasizes, through the dP_T/dt term, the role of curvature of the potential profile in addition to the usual emphasis on depth of the potential minimum when considering membrane interactions.

The authors acknowledge useful discussions with Dr. D. Gallez. N. E. Thomas was supported by a SERC CASE studentship with Unilever, U.K. The interest and support of Dr. G. Akay and Prof. H. Barnes of Unilever Research, Port Sunlight, are appreciated. The authors are grateful to Ms. C. Winters and Mr. M. Turner for the electron micrographs.

REFERENCES

Baker, A. J., W. T. Coakley, and D. Gallez. 1993. Influence of polymer concentration and molecular weight and of enzymic glycocalyx modification on erythrocyte interaction in dextran solutions. *Eur. Biophys. J.* 22:53–62.

Baumler, H., and E. Donath. 1987. Does dextran indeed significantly increase the surface potential of human red blood cells? *Stud. Biophys.* 120:113–122.

Brochard, F., and J. F. Lennon. 1975. Frequency spectrum of flicker phenomenon in erythrocytes. *J. Physique.* 36:1035–1047.

Brooks, D. E. 1973a. The effect of neutral polymers on the electrokinetic potential of cells and other charged particles. II. *J. Colloid Interface Sci.* 43:687–699.

Brooks, D. E. 1973b. The effect of neutral polymers on the electrokinetic potential of cells and other charged particles. III. Experimental studies on the dextran/erythrocyte system. *J. Colloid Interface Sci.* 43:700–713.

Buxbaum, K., E. A. Evans, and D. E. Brooks. 1982. Quantitation of surface affinities of red blood cells in dextran solutions and plasma. *Biochemistry.* 21:3235–3239.

Chien, S., S. Simchon, R. E. Abbott, and K.-M. Jan. 1977. Surface adsorption of dextrans on human red blood cell membrane. *J. Colloid Interface Sci.* 62:461–470.

Coakley, W. T., H. Darmani, and A. J. Baker. 1991. Membrane contact induced between erythrocytes by polycations, lectins and dextran. *In* Cell and Model Membrane Interactions. S. Ohki, editor. Plenum Press, New York. 25–46.

Coakley, W. T., and D. Gallez. 1989. Membrane-membrane contact: Involvement of interfacial instability in the generation of discrete contacts. *Biosci. Rep.* 9:675–691.

Coakley, W. T., D. Gallez, N. E. Thomas, and A. J. Baker. 1994. An interfacial instability approach to erythrocyte adhesion by macromolecules. *Colloids Surfaces B: Biointerfaces.* 2:281–290.

Coakley, W. T., L. A. Hewison, and D. Tilley. 1985. Interfacial instability and the agglutination of erythrocytes by polylysine. *Eur. Biophys. J.* 13:123–130.

Coakley, W. T., N. E. Thomas, and D. Gallez. 1994. An interfacial instability approach to erythrocyte adhesion by macromolecules. *Colloids Surfaces B: Biointerfaces.* 2:281–290.

Dan, J. C. 1967. Acrosome reaction and lysins. *In* Fertilisation, Vol. 1. C. B. Metz, and A. Monroy, editors. Academic Press, New York. 237–283.

Darmani, H., and W. T. Coakley. 1990. Membrane-membrane interactions: parallel membranes or patterned discrete contacts. *Biochim. Biophys. Acta.* 1021:182–190.

Dimitrov, D. S. 1982. Instability of thin liquid films between membranes. *Colloid Polymer Sci.* 260:1137–1144.

Donath, E., L. Pratsch, H.-J. Baumler, A. Voigt, and M. Teager. 1989. Macromolecule depletion at membranes. *Stud. Biophys.* 130:117–122.

Donath, E., and A. Voigt. 1983. Charge distribution within cell surface coats of single and interacting surfaces—a minimum free electrostatic energy approach. Conclusions for electrophoretic mobility measurements. *J. Theor. Biol.* 101:569–584.

Doulah, F. A., W. T. Coakley, and D. Tilley. 1984. Intrinsic electric fields and membrane bending. *J. Biol. Phys.* 12:44–51.

Evans, E. A. 1983. Bending elastic modulus of red cell membranes derived from buckling instability in micropipette aspiration experiments. *Biophys. J.* 43:27–30.

Evans E. A. 1985. Detailed mechanics of membrane-membrane adhesion and separation. 1. Continuum of molecular cross-bridges. *Biophys. J.* 48:175–183.

Fisher, L. 1993. Forces between biological surfaces. *Chem. Soc. Faraday Trans.* 89:2567–2582.

Francis, G. W., L. R. Fisher, R. A. Gamble, and D. Gingell. 1987. Direct measurement of cell detachment force on single cells using a new electromechanical method. *J. Cell Sci.* 87:519–523.

Freedman, J. C., and P. C. Laris. 1981. Electrophysiology of cells and organelles—studies with optical potentiometric indicators. *In* International Review of Cytology, Supplement 12. A. L. Muggleton-Harris, editor. Academic Press, New York. 177–246.

Gallez, D. 1994. Non-linear stability analysis for animal cell adhesion to solid support. *Colloids Surfaces B: Biointerfaces.* 2:273–280.

Gallez, D., and W. T. Coakley. 1986. Interfacial instability at cell membranes. *Prog. Biophys. Mol. Biol.* 48:155–199.

Glaser, R. 1982. Echinocyte formation induced by potential changes of human red blood cells. *J. Membr. Biol.* 66:79–85.

Haydon, D. A., and G. V. F. Seaman. 1967. Electrokinetic studies on the ultrastructure of the human erythrocyte I. *Arch. Biochem. Biophys.* 122:126–136.

Hiemenz, P. C. 1986. Principles of Colloid and Surface Chemistry. Marcel Dekker, New York. 815 pp.

Hoffman, J. F., and P. C. Laris. 1974. Determination of membrane potentials in human and amphiuma red blood cells by means of a fluorescent probe. *J. Physiol. (Lond.).* 239:519–552.

Israelachvili, J. N., and P. M. McGuigan. 1988. Forces between surfaces in liquids. *Science.* 241:795–800.

Ivanov, I. B. 1980. Effect of surface mobility on the dynamic behaviour of thin liquid films. *Pure Appl. Chem.* 52:1241–1262.

Ivanov, I. B., and D. S. Dimitrov. 1974. Hydrodynamics of thin liquid films: effect of surface viscosity on thinning and rupture of foam films. *Colloid Polymer Sci.* 252:982–990.

Jan, K.-M. 1979. Role of hydrogen bonding in red cell aggregation. *J. Cell Physiol.* 101:49–55.

Jan, K.-M., and S. Chien. 1973a. Role of surface electric charge in red blood cell interactions. *J. Gen. Physiol.* 61:638–654.

Jan K.-M., and S. Chien. 1973b. Influence of the ionic composition of fluid medium on red cell aggregation. *J. Gen. Physiol.* 61:655–668.

Katchalsky, A., D. Danon, A. Nevo, and A. de Vries. 1959. Interaction of basic polyelectrolytes with the red blood cell 2. Agglutination of red blood cells by polymeric bases. *Biochim. Biophys. Acta.* 33:120–138.

Levine, S., M. Levine, K. A. Sharp, and D. E. Brooks. 1983. Theory of the electrokinetic behaviour of human erythrocytes. *Biophys. J.* 42:127–135.

Lipowsky R. 1995. Generic interactions of flexible membranes. *In* Structure and Dynamics of Membranes. Handbook on Physics of Biological Systems, Vol. 1. R. Lipowsky and E. Sackmann, editors. Elsevier, Amsterdam.

Luckham, P. F., and Ansarifar, M. A. 1990. Biomedical aspects of the direct measurements of the forces between adsorbed polymers and proteins. *Br. Polym. J.* 22:233–243.

Luckham, P. F., and Klein. 1990. Forces between mica surfaces bearing adsorbed homopolymers in good solvents: the effect of bridging and dangling tails. *J. Chem. Soc. Faraday Trans.* 86:1363–1368.

Marra, J., and M. L. Hair. 1988. Forces between two poly(2-vinylpyriine)-covered surfaces as a function of ionic strength and polymer charge. *J. Phys. Chem.* 2:6044–6051.

McIver, D. J. L., and S. Schurch. 1982. Interfacial free energies of intact and reconstituted erythrocyte surfaces: implication for biological adhesion. *Biochim. Biophys. Acta.* 691:52–60.

Miller, C. A. 1978. Stability of interfaces. *In* Surface and Colloid Science, Vol. 10. E. Matijevic, editor. Plenum Press, New York. 227–293.

Patel, S. S., and M. Tirrell. 1989. Measurement of forces between surfaces in polymer fluids. *Annu. Rev. Phys. Chem.* 40:597–635.

Peterson, M. A., H. Strey, and E. Sackmann. 1992. Theoretical and phase contrast microscopic eigenmode analysis of erythrocyte flicker amplitudes. *J. Phys. II France.* 2:1273–1285.

Prevost, M., and D. Gallez. 1984. The role of repulsive hydration forces on the stability of aqueous black films. *J. Chem. Soc. Faraday Trans. II.* 80:517–533.

Prevost, M., Gallez, D., and Sanfeld, A. 1983. Electrodynamic stability of unsymmetrical aqueous films; application to membrane-membrane interactions. *J. Chem. Soc. Faraday Trans. II.* 79:961–976.

Rossi, G., and P. A. Pincus. 1988. Interactions between unsaturated-polymer adsorbed surfaces. *Europhys. Lett.* 5:641–646.

Ruchenstein, E., and R. K. Jain. 1974. Spontaneous rupture of thin-liquid films. *J. Chem. Soc. Faraday Trans. II.* 70:132–147.

Russell, L., R. Petersen, and M. Freud. 1979. Direct evidence for formation of hybrid vesicles by fusion of plasma and outer acrosomal membranes in boar spermatozoa. *J. Exp. Zool.* 208:41–56.

Schnebli, H. P., C. Roeder, and L. Tarcsay. 1976. Reaction of lectins with human erythrocytes. *Exp. Cell Res.* 98:273–276.

Skalak, R., P. R. Zarda, K.-M. Jan, and S. Chien. 1981. Mechanics of rouleaux formation. *Biophys. J.* 35:771–781.

Snabre, P., G. H. Grossman, and P. Mills. 1985. Effects of dextran polydispersity on red blood cell aggregation. *Colloid Polym. Sci.* 263: 478–483.

Snowden, M. J., S. M. Clegg, and P. A. Williams. 1991. Flocculation of silica particles by adsorbing and non-adsorbing polymers. *J. Chem. Soc. Faraday Trans.* 87:2201–2207.

Sung, L. A., and E. A. Kabat. 1994. Agglutination-induced erythrocyte deformation by two blood group A-specific lectins: studies by light and electron microscopy. *Biorheology.* 31:353–364.

Sutherland, W. H., and J. A. V. Pritchard. 1979. An improved apparatus for micro-electrophoresis. *In* Cell Electrophoresis: Clinical Applications and Methodology. A. W. Preece and D. Sabolovic, editors. Elsevier/ North Holland, Amsterdam. 421–430.

Thomas, N. E., W. T. Coakley, and G. Akay. 1993. The lateral separation of contacts on erythrocytes agglutinated by polylysine. *Cell Biophys.* 20:125–147.

van Oss, C. J., K. Arnold, and W. T. Coakley. 1990. Depletion flocculation and depletion stabilisation of erythrocytes. *Cell Biophys.* 17:1–11.

Viitala, J., and J. Jarnefelt. 1985. The red cell surface revisited. *Trends Biochem. Sci.* 10:392–395.

Vincent, B., J. Edwards, S. Emmett, and A. Jones. 1986. Depletion flocculation in dispersions of sterically stabilized particles (soft spheres). *Colloids Surf.* 18:261–281.

Vink, H. 1971. Precision measurements of osmotic pressure in concentrated polymer solutions. *Eur. Polym. J.* 7:1411–1419.

Ward, M. D., and D. A. Hammer. 1992. Morphology of cell-substratum adhesion: influence of receptor heterogeneity and nonspecific forces. *Cell Biophys.* 20:177–222.

Wendel, H., D. Gallez, and P. M. Bisch. 1981. On the dynamic stability of fluid dielectric films. *J. Colloid Interface Sci.* 84:1–7.